NASA TECHNICAL MEMORANDUM

NASA TM X-2322

NASA TM X-2322

EVALUATION OF NOVEL DEPRESSED COLLECTOR FOR LINEAR-BEAM MICROWAVE TUBES

by Francis E. Kavanagh, Robert E. Alexovich, and Gerald J. Chomos

Lewis Research Center
Cleveland, Ohio 44135

NATIONAL AERONAUTICS AND SPACE ADMINISTRATION • WASHINGTON, D. C. • AUGUST 1971

1. Report No.	2. Government Accession No.	3. Recipient's Catalog No.
NASA TM X-2322		

4. Title and Subtitle	5. Report Date
EVALUATION OF NOVEL DEPRESSED COLLECTOR FOR LINEAR-BEAM MICROWAVE TUBES	August 1971
	6. Performing Organization Code

7. Author(s)	8. Performing Organization Report No.
Francis E. Kavanagh, Robert E. Alexovich, and Gerald J. Chomos	E-6224
	10. Work Unit No. 164-21

9. Performing Organization Name and Address	11. Contract or Grant No.
Lewis Research Center National Aeronautics and Space Administration Cleveland, Ohio 44135	
	13. Type of Report and Period Covered: Technical Memorandum

12. Sponsoring Agency Name and Address	14. Sponsoring Agency Code
National Aeronautics and Space Administration Washington, D.C. 20546	

15. Supplementary Notes

16. Abstract

Laboratory evaluation tests were conducted at Lewis Research Center on a novel depressed collector for linear beam microwave tubes. The objective of these tests is to demonstrate the feasibility of increasing the efficiency of microwave tubes, having a large axial and radial velocity spread in the spent beam, using a novel collector design. The first iteration yielded a collector efficiency of 57 percent on an electrostatically focused klystron. Previous to this work, conventional depressed collector efficiencies on tubes having similar velocity distribution have been in the order of 25 to 38 percent. Improved designs are expected to raise collector efficiencies to 75 percent or more and promise to significantly improve the overall efficiencies of linear beam microwave tubes without the adverse effects experienced with previous collector designs.

17. Key Words (Suggested by Author(s))	18. Distribution Statement
Microwave tubes High-efficiency multistaged depressed collector	Unclassified - unlimited

19. Security Classif. (of this report)	20. Security Classif. (of this page)	21. No. of Pages	22. Price*
Unclassified	Unclassified	24	$3.00

*For sale by the National Technical Information Service, Springfield, Virginia 22151

EVALUATION OF NOVEL DEPRESSED COLLECTOR FOR LINEAR-BEAM MICROWAVE TUBES

by Francis E. Kavanagh, Robert E. Alexovich, and Gerald J. Chomos

Lewis Research Center

SUMMARY

Laboratory evaluation tests were conducted at Lewis Research Center on a novel depressed collector for linear beam microwave tubes. The objective of these tests is to demonstrate the feasibility of increasing the efficiency of microwave tubes, having a large axial and radial velocity spread in the spent beam, using a novel collector design. The first iteration yielded a collector efficiency of 57 percent on an electrostatically focused klystron. Previous to this work, conventional depressed collector efficiencies on tubes having similar velocity distribution have been in the order of 25 to 38 percent. Improved designs are expected to raise collector efficiencies to 75 percent or more and promise to significantly improve the overall efficiencies of linear beam microwave tubes without the adverse effects experienced with previous collector designs.

INTRODUCTION

Advanced communication satellites are expected to use microwave tubes with output powers of 1 kilowatt and greater. One of the most difficult and important problems in the design of microwave tubes for space applications is the task of obtaining the highest possible efficiency. An efficient device requires less prime power. This results in decreased cost and weight of the solar array. In addition an efficient tube will result in decreased weight and size of the thermal control system.

High frequency space communications require linear beam microwave tubes for power generation. Linear beam tubes all possess a common geometry in which an electron beam is formed from a convergent gun, a radiofrequency (rf) signal interacts with the beam converting kinetic energy to rf energy, and rf energy is extracted from an output cavity. The tubes differ only in their method of beam confinement (i.e., either electrostatic lenses or magnetic fields) and the type of beam rf interaction (standing wave interaction for klystrons and traveling field interaction for TWT's). The electron beam after conversion of kinetic energy to rf energy is made up of electrons having

velocities which range from near zero to approximately twice their initial velocity. Efficient collection of beams having large axial and radial velocity spread is difficult and is the major obstacle in achieving the highest possible efficiency from microwave tubes.

One way to improve efficiency in microwave tubes is to convert the kinetic energy of the electron beam into potential energy after it has passed through the rf interaction region. This can be done by collector depression. To date, conventional depressed collectors have yielded only moderate improvements in the overall efficiency of microwave tubes. Their basic deficiency was a premature onset of reflected primary and secondary electrons which backstreamed into the tube at modest levels of depression causing noise and instability.

The Lewis Research Center is currently studying the characteristics of an analytical design developed at the Center. This design promises a substantial increase in overall efficiency by maximizing the efficiency of the collection process. In parallel attempts to obtain high efficiency tubes for space applications, Lewis is also pursuing an active contractual program. The General Electric Company has conducted under contract NAS3-11532 an analytic and experimental program to apply an electrostatic depressed collector to an 850-megahertz klystron (ref. 1). Under contract NAS 3-11530, General Electric has performed an analytic study of depressed collectors specifically excluding the electrostatic type (ref. 2). Hughes Aircraft Company under contract NAS3-11536 is conducting an analytic and experimental program to apply a depressed collector to a 10 gigahertz TWT.

The work described in this report was performed to experimentally verify an analytical design, described in reference 3, that promises a substantial increase in overall efficiency by maximizing the efficiency of the collector process. The tests were conducted on an electrostatically focused klystron (ESFK) whose output power was varied from zero to saturation (890 W). An eight-stage depressed collector was used. The tube was tested with and without a depressed collector. During depressed collector operation, the voltages on the depressed collector electrodes were varied by ±10 percent.

DESCRIPTION OF COLLECTOR OPERATION

The depressed collector has three functions which are: (1) to sort electrons according to their velocity, (2) to slow the electrons so they may be collected with the lowest velocity possible, and (3) to prevent backstreaming of electrons, both reflected primaries and secondaries, into the circuit region of the tube.

The Lewis Research Center concept is derived from a hypothetical spherical surface enclosing the collector region together with a central cone and spike. A continuous

distribution of the potential along the hypothetical spherical surface is chosen so that the collector operates with the highest possible efficiency. The cone and the spike are assumed to be at the potential $-1.5\ V_0$, where V_0 is the body potential with respect to the cathode. In any tube considered for future applications only a few electrons will have energies larger than $1.5\ V_0$. Thus, only a few electrons will impinge on the spike and cone.

Figure 1 shows the equipotential lines and electron trajectories within the hypothetical sphere enclosing the collector region where α_f is the entrance angle of the electron trajectories depicted and V_i is the injection energy of the electrons. It is known that a metallic conductor can be inserted into an electric field and this action will not disturb the original field configuration as long as it is placed along an equipotential surface. Therefore, electrodes were fabricated in the shape of the equipotential surfaces, within the sphere, that result from the surface potential distribution. This produces the same potential distribution within the collector region as obtained by using the sphere and also provides a geometry that permits the collection of electrons.

The electron trajectories in figure 1 represent the motion of a spent electron beam. Electrons with the same kinetic energy enter the collector with different angles, radial

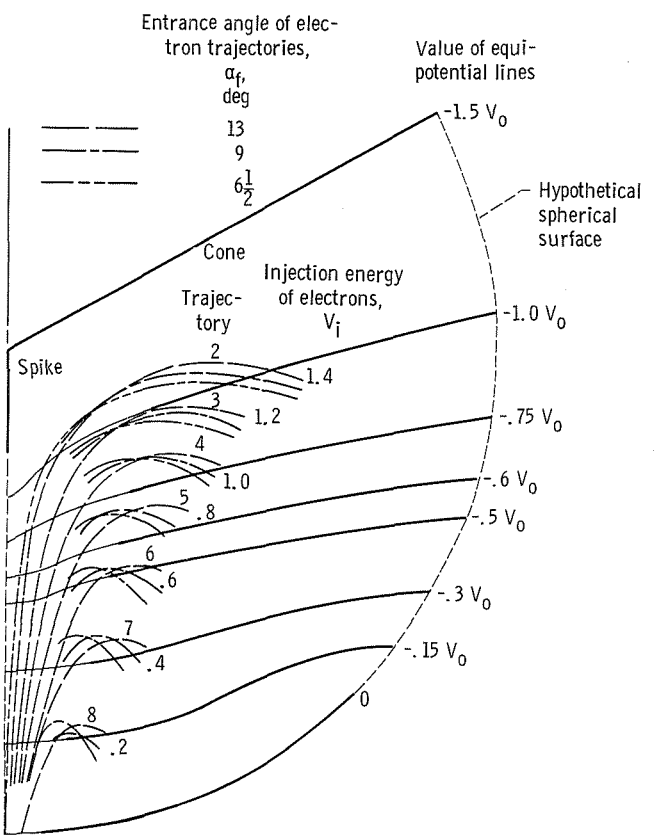

Figure 1. -Electron trajectories within Lewis depressed collector.

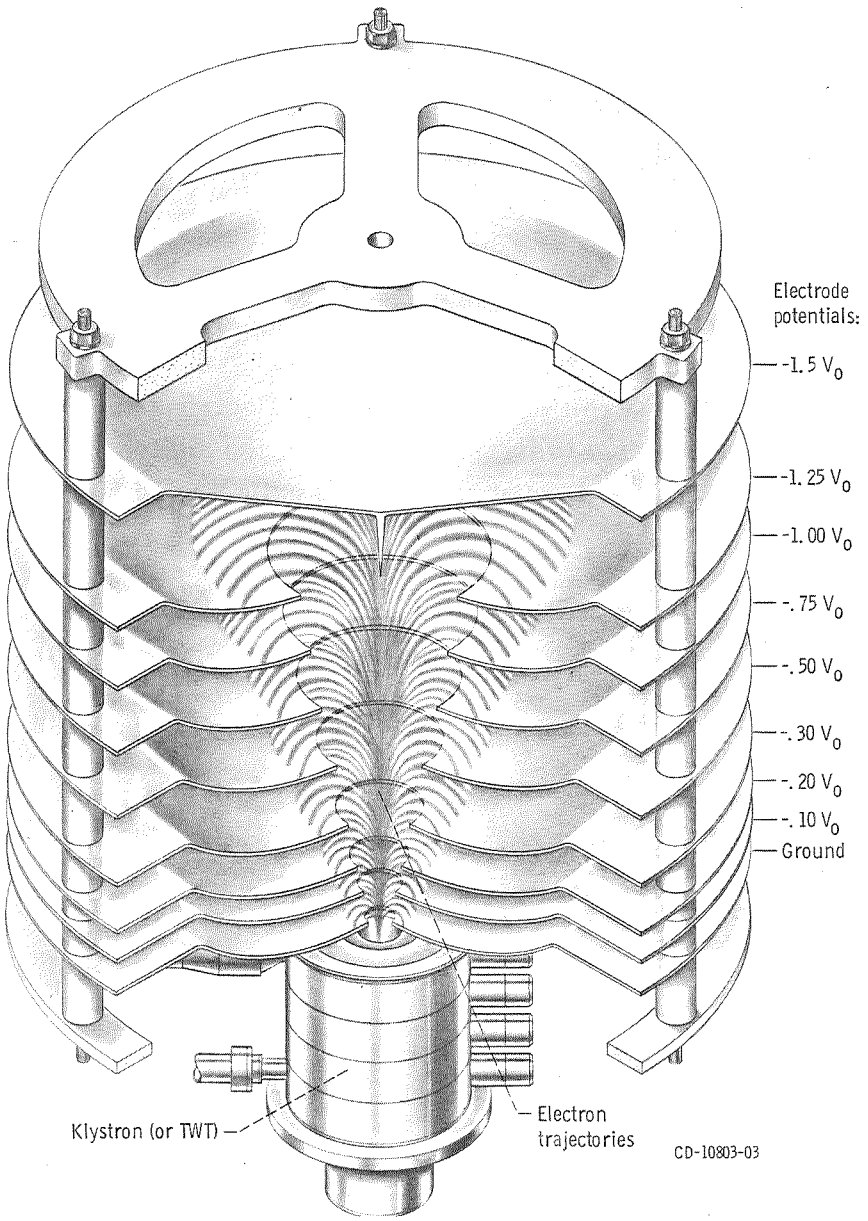

Figure 2. - Artist's drawing of depressed collector concept. V_0 = |Voltage on cathode with respect to ground|.

velocities, and radial positions. This prevents the collection of these electrons at the same point with minimum velocity. Therefore, they will not be collected on the same collector electrode. If the beam radius at entry is made small compared to the distance the electrons travel in the collector region, the factor of radial distribution is negated.

In the present collector configuration the short spike acts on the more energetic electrons while the remainder of the electrons are acted on mainly by fields in the vicinity of the entrance. For high collector efficiency, as little energy as possible should be expended in obtaining the optimum radial deflection.

Backstreaming of electrons into the rf interaction region of the tube result from reflected primaries and/or emitted secondary electrons. The design of the collector produces an electric field within the collector region which diverges primary electrons from the tube axis. This prevents backstreaming of primary electrons. The designed aperture sizes and locations cause primary electrons to be collected on the upper side of the electrodes. A negative electric field in the region suppresses secondary electron emission. Figure 2 depicts an artist's drawing of the concept discussed previously.

EXPERIMENTAL APPARATUS

Collector Fabrication

All collector electrodes were formed from OFHC copper by a spinning process. The spinning mandrels were machined from aluminum to contours which were obtained from a computer plot of equipotential surfaces. Electrodes were separated from one another by insulators made of boron nitride. The entire assembly was held together by three through bolts which fit into steel endplates. Each through bolt was covered with an alumina sleeve that fits inside the boron nitride insulators. This sleeve was found to be necessary to prevent voltage breakdown between the highly negative electrodes and the grounded endplates and bolts. Figure 3 depicts the assembly of the first seven electrode plates. Figure 4 shows the eighth electrode which is in the shape of a cone with protruding spike.

All electrodes except the top and bottom possess "patches" which measured current to the underside of the electrodes as depicted in figure 5. The patches are flame sprayed copper over an insulating substrate of aluminum oxide. The patches are held at the same potential as the electrode so as not to disturb the potential distribution but they are electrically isolated to permit current measurement. Finally, after masking the periphery of the patches, the interior surface of each electrode was blackened with soot from an acetylene torch. This coating was applied to reduce secondary emission caused by electrons striking the electrodes.

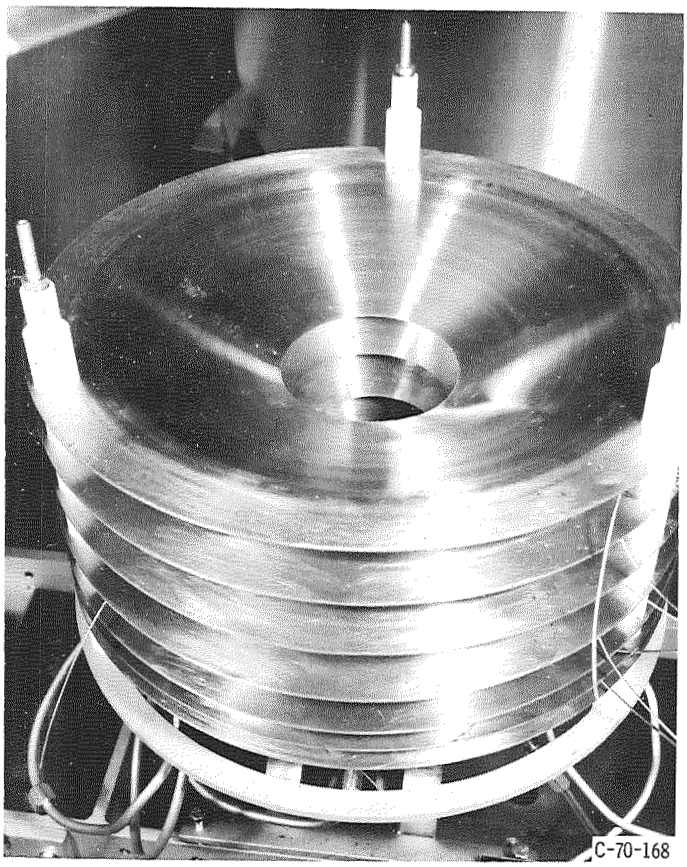

Figure 3. - Electrode assembly. (Electrodes 1 to 7.)

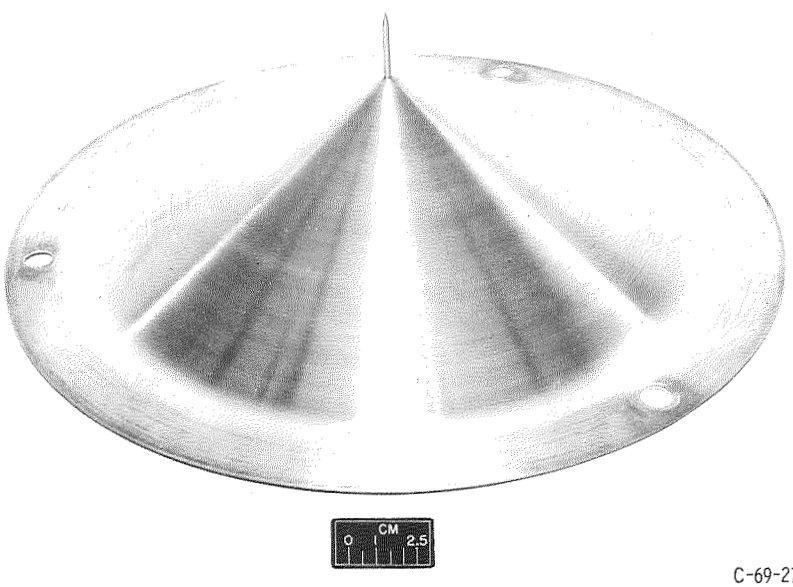

Figure 4. - Cone-shaped electrode with spike.

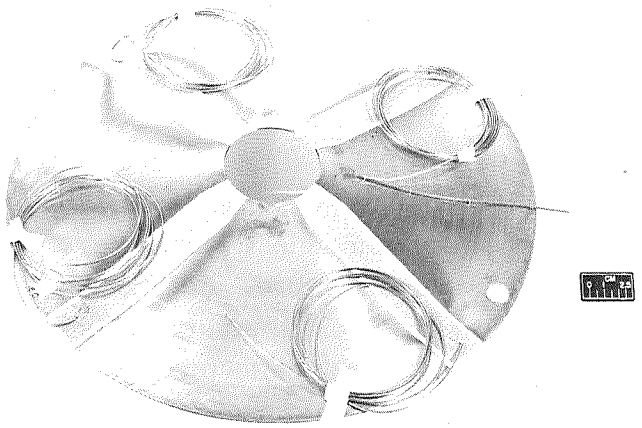

C-69-3009

Figure 5. - Collector electrode showing "patches" and thermocouple.

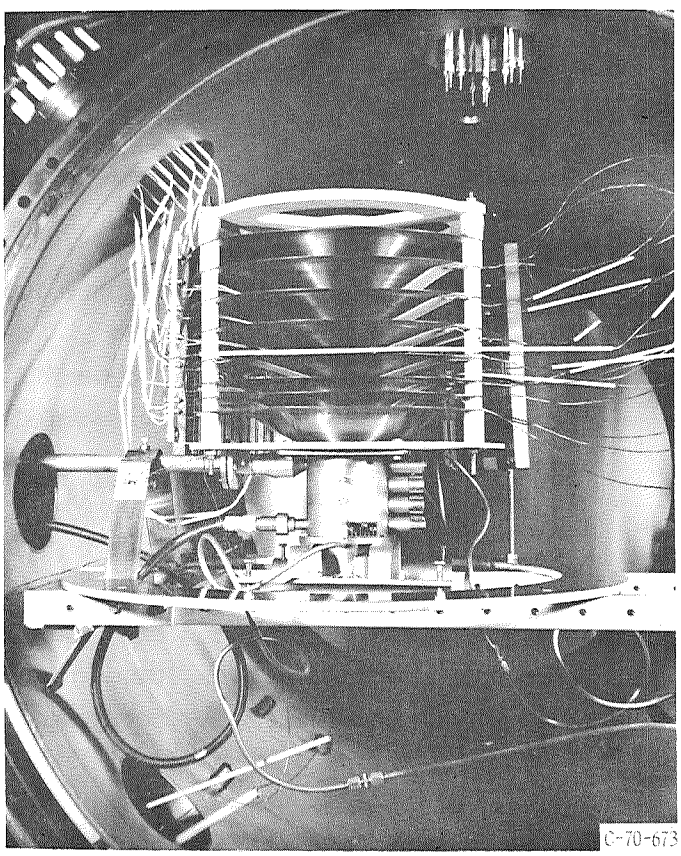

C-70-673

Figure 6. - Klystron and depressed collector in vacuum chamber.

Figure 6 depicts the klystron and depressed collector assembled and installed in the vacuum chamber in which it was tested. The collector was assembled without the top or spike electrode and the hole concentricity was checked with a gage block. With the collector in place, the top electrode was put in place and the spike alined with the tip of a rod inserted through the tube from the cathode end. The final step in the procedure was to mechanically install and electrically connect the cathode. In figure 6 one can see the input and output rf coax lines on the left side of the picture. Also depicted in the picture are the numerous electrical and thermocouple connections.

The system was radiantly heated, using electrical heaters, to a temperature of 400° C and baked for 4 hours at that temperature. Adsorbed and entrapped gases were driven off during this bakeout which enabled an operating pressure of 1×10^{-9} torr to be achieved. During all subsequent testing, the collector electrodes were heated to approximately 300° C and maintained at this temperature. This was found to be necessary to prevent breakdown of adsorbed gases released by electron bombardment of the soot coated collector electrodes.

The cathode was activated by raising the cathode temperature to its operating point over a period of from 2 to 4 hours and slowly increasing beam voltage and current. The type of cathode used was a tungsten matrix impregnated with a barium-calcium-aluminate mixture.

Tube Description

The tube used for the present investigation is an electrostatically focused klystron (ESFK), the Litton Industries L-5101. It was modified to have a removable collector and a replaceable cathode. Cathode current is 0.380 ampere at 7 kilovolts. The klystron had a saturated power output P_o of 890 watts, a 3-decibel bandwidth of 7.5 megahertz and a center frequency of 2.25 gigahertz. Saturated gain was 37 decibels.

Vacuum System

The vacuum system is a completely oil free system consisting of sorption pumps for fore pumping, ion pumps for primary pumping, and titanium sublimation auxiliary pumps. The system is capable of being baked out at temperatures up to 250° C. The vacuum chamber as depicted in figure 7 is a cylinder 1.07 meters in diameter and 1.8 meters long. On the periphery of the chamber are seven 0.152-meter ports used for, dc voltage, rf input and output power, collector instrumentation, and water cooling feedthroughs. One end of the chamber is a completely removable door with castered

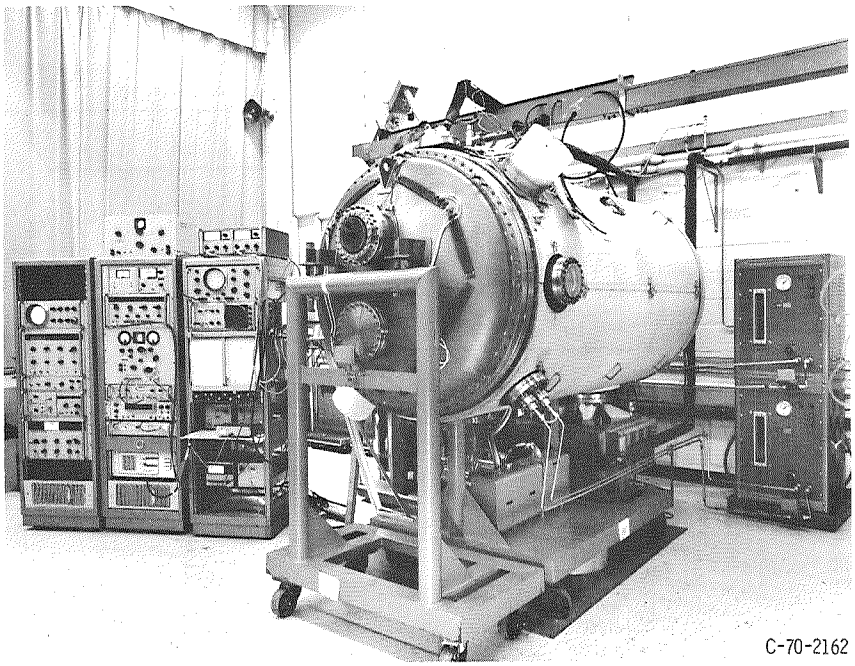

Figure 7. - Vacuum chamber.

cart. On this door are two 0.203-meter ports. All parts of the chamber are made of nonmagnetic stainless steel.

The fore pumping is accomplished by a battery of sorption pumps capable of roughing the vacuum chamber (with tube assembly) to 3 microns in $1\frac{1}{2}$ hours. The primary pumps are ion pumps having the following pumping speeds: nitrogen, 1.5 cubic meters per second; argon, 0.095 cubic meter per second; and helium, 0.220 cubic meter per second. A 40-cubic-meter-per-second auxiliary titanium sublimation pump is also available.

The vacuum chamber is equipped with a Helmer type vacuum gage. During operation of the tube, the pressure in the tube area is typically 1×10^{-8} torr. At the present time, it is possible to assemble the demountable tube, install it in the chamber, and start the ion pumps within 8 hours.

Power Supplies

Operating voltages for the tube and collector were obtained from four power supplies (see fig. 8). The heater supply was an isolated supply which provided regulated dc power to heat the cathode. The cathode supply provided the necessary power for operation of the tube.

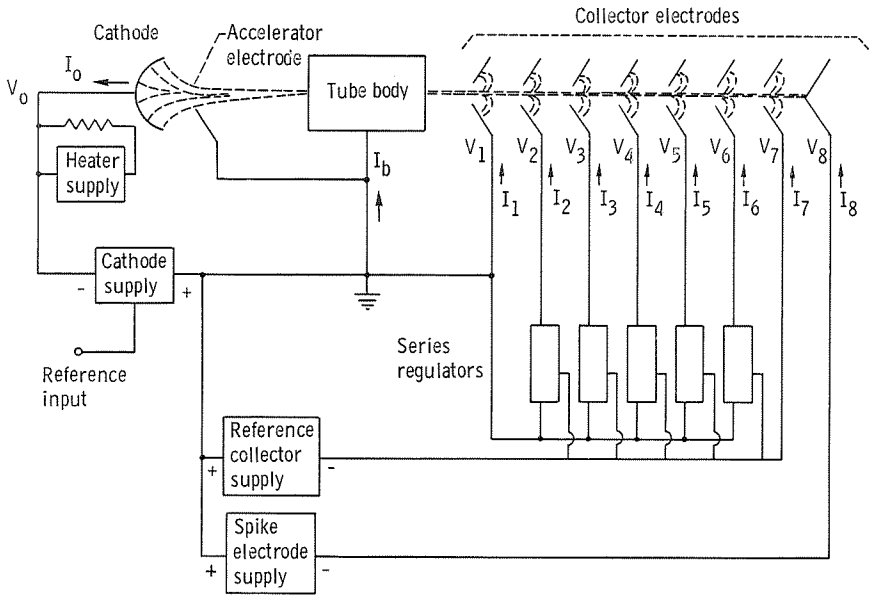

Figure 8. - Direct current test setup.

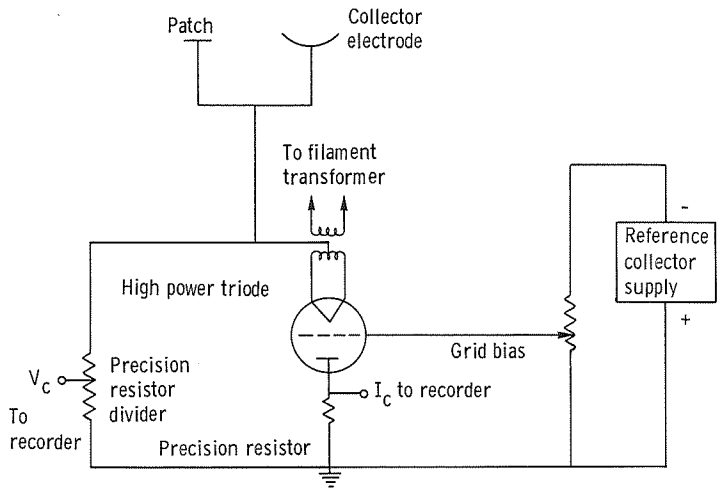

Figure 9. - Series regulator circuit.

The reference collector supply was used to establish the operating potential for electrode 7 and also was used as a reference for the series regulator circuits shown in figure 9. Operating voltages for electrodes 2 to 6 were derived as fractions of the reference voltage supply using series regulators set to the desired potential.

Characteristics of the aforementioned power supplies are shown in table I.

TABLE I. - POWER SUPPLY SPECIFICATIONS

Supply	Voltage range, V	Current range, A	Peak to peak full-scale output, percent	Regulation full-scale output, percent
Spike electrode	0 to 20 000	0 to 0.1	0.01	0.01
Reference collector	0 to 15 000	0 to 2	.01	.1
Cathode	0 to 10 000	0 to 1	.1	.1
Heater	0 to 15	0 to 15	1	1.0

Direct Current Instrumentation

The dc measurements required for the collector evaluation are described as follows. All voltage measurements were derived from precision resistor networks connected to each potential. The output from these networks was a 0- to 5-volt dc signal proportional to the voltage being measured. This signal was used as the input to a strip-chart recorder to form a permanent record of the measurements.

Currents to the patches on the lower side of electrodes 2 to 7 were measured by means of an isolated current probe which senses the magnetic field produced by current in a conductor. A wire attached to each patch was placed through the current sensor and then connected to the series regulator outside the vacuum tank. The output of each current probe is a 0- to 5-volt signal, proportional to the measured current. This was used as the input to a strip-chart recorder. This technique enabled the patch and electrode to be at the same electrical potential but allowed current flowing to the patch to be measured independently from the total electrode current.

Collector electrode currents were determined by either current probes similar to the ones described previously or by measuring the voltage across a precision resistor inserted in the ground side of a series regulator circuit. In either case a voltage proportional to the current being measured was again used as the input to a recorder.

TEST PROCEDURE

Tests were made of the tube and collector performance for power output levels from zero to saturation. A continuous set of data was obtained by using a function generator to amplitude modulate the input drive signal. Steady-state test data were also taken at constant power output levels. The voltages on the plates were varied by ±10 percent about nominal voltages in order to maximize the collector efficiency at saturated power output.

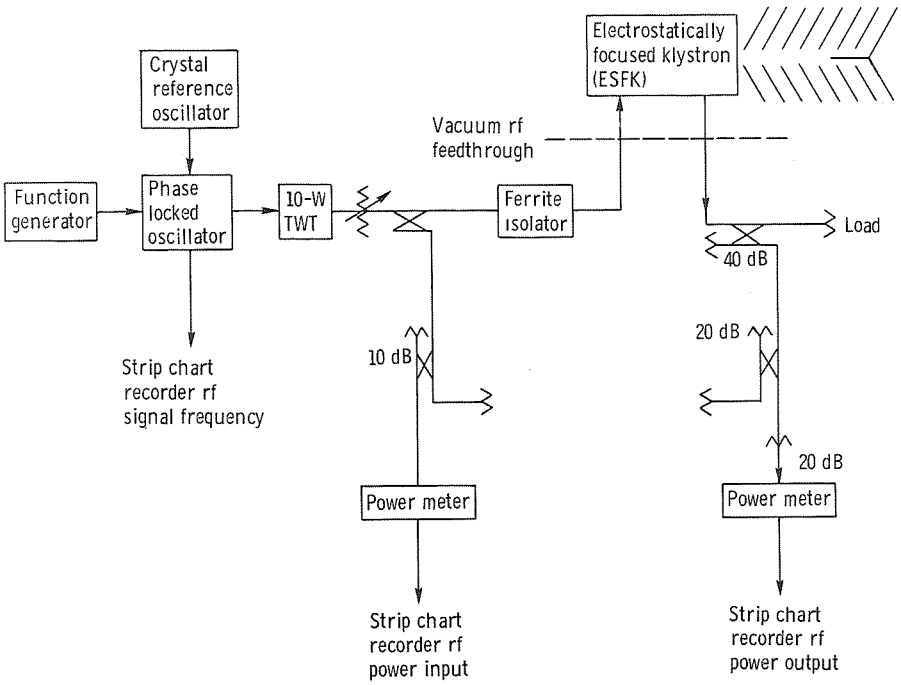

Figure 10. - Radiofrequency test setup.

During all rf testing, the following dc measurements were made: collector voltages, collector currents, collector patch currents, body current, cathode current, and cathode voltage. The test setup used for rf tests is shown in figure 10. A crystal controlled phased locked oscillator was used to drive a 10-watt TWT. This was used as a continuous wave signal source during rf testing. An isolator, located between the signal source and test klystron, was used to minimize voltage reflections due to small mismatches in the signal input line. The output of the klystron was dissipated in a water load outside the vacuum chamber.

Radiofrequency power measurements were made calorimetrically in the water load and also by using self-balancing bolometer-type power meters with recorder outputs. A narrow band (10-kc) spectrum analyzer with CRT display was utilized to determine if noise or spurious signals were present in the tube output. Also, noise spectrums of the output signal were determined using the test setup shown in figure 11. The output signal from the klystron and a reference signal from the input signal source were fed into a discriminator. A phase shifter in the reference line permitted adjustment to be made in the reference signal phase. AM and FM noise spectrums were measured by setting the reference signal phase to be in-phase or in quadrature phase, respectively, with respect to the output signal. The resultant noise spectrum was measured using a wave analyzer.

Voltage standing wave ratio (VSWR) of the output line, loss of passive rf components

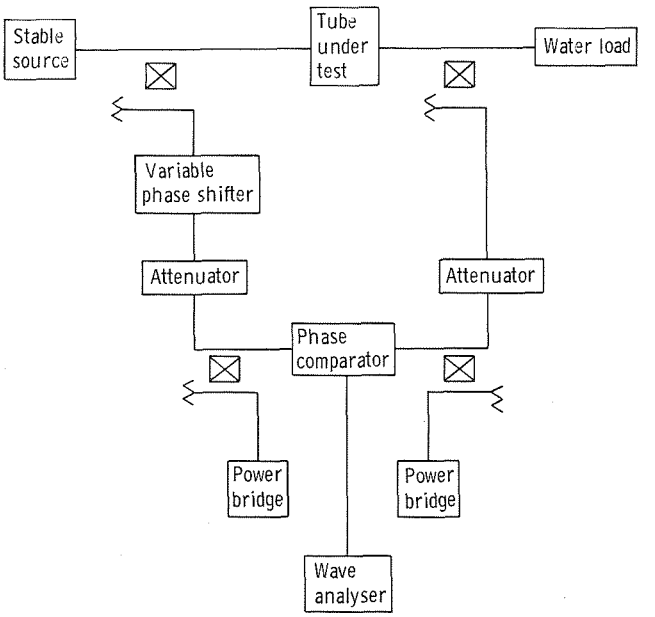

Figure 11. - AM and FM noise measurement test setup.

in the input and output circuits, and phase shift through the klystron were measured with a network analyzer.

With the signal source oscillator unlocked, the operating center frequency of the tube was determined. Gain and phase measurements were made at several input power levels by sweeping the input signal frequency through the operating band of the tube and recording frequency, input and output power and change of phase.

RESULTS AND DISCUSSION

Current Distribution to Collector Electrodes

Figure 12 illustrates the variation in collector currents caused by varying the input power. These data were taken by amplitude modulating the input drive signal to produce a variation in output power P_o from zero to saturation (890 W) and back to zero.

The extreme left of the figure at time equal 0 represents the current distribution in the collector under dc conditions, that is, without rf on the beam. Under these conditions, the electron velocities at the entrance to the collector are determined by the beam accelerating voltage and space charge forces. In the case shown, 92 percent of the beam goes to plate 5 under dc conditions. The velocities of the electrons entering the collector region are changed as the beam is modulated and power is extracted from the beam in the form of rf power. As the rf output power is increased, the velocity of the

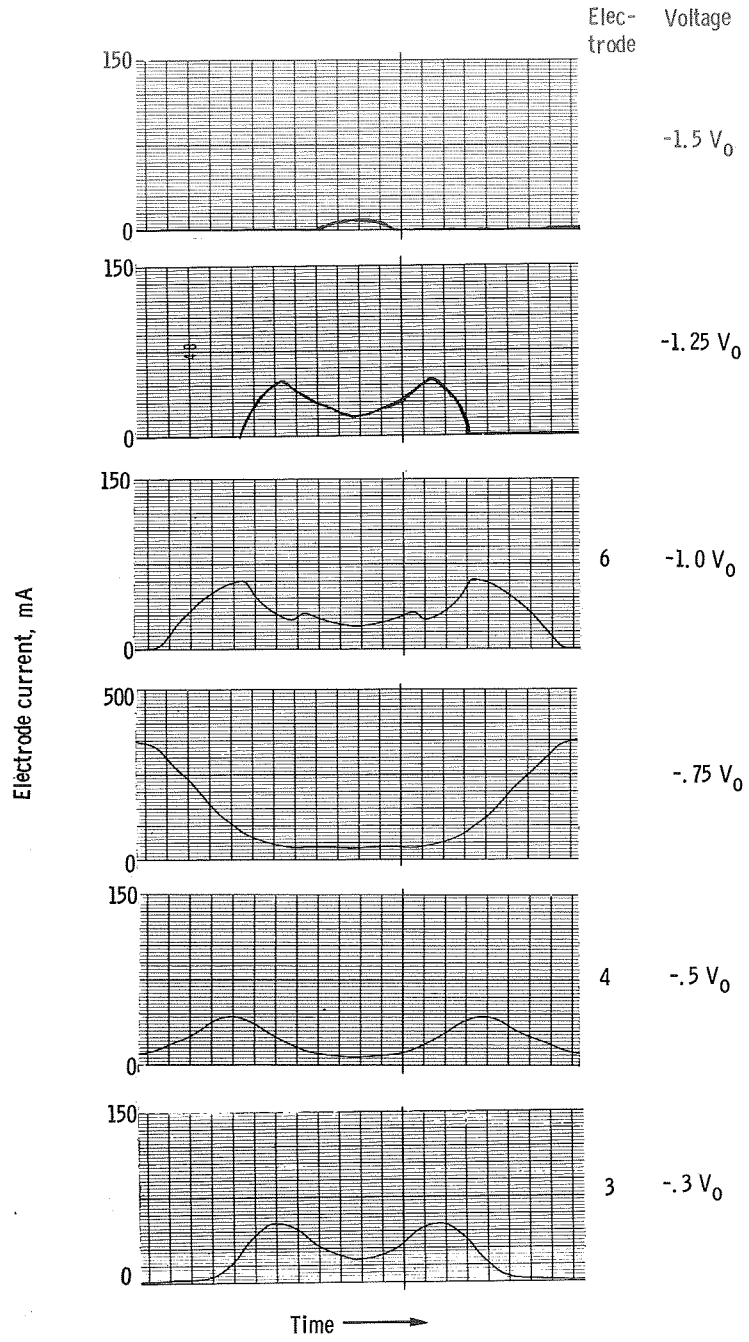
Elec-
trode
Voltage
150
0
-1.5 V_0
150
0
-1.25 V_0
150
0
6
-1.0 V_0
500
0
-.75 V_0
150
0
4
-.5 V_0
150
0
3
-.3 V_0
Electrode current, mA
Time

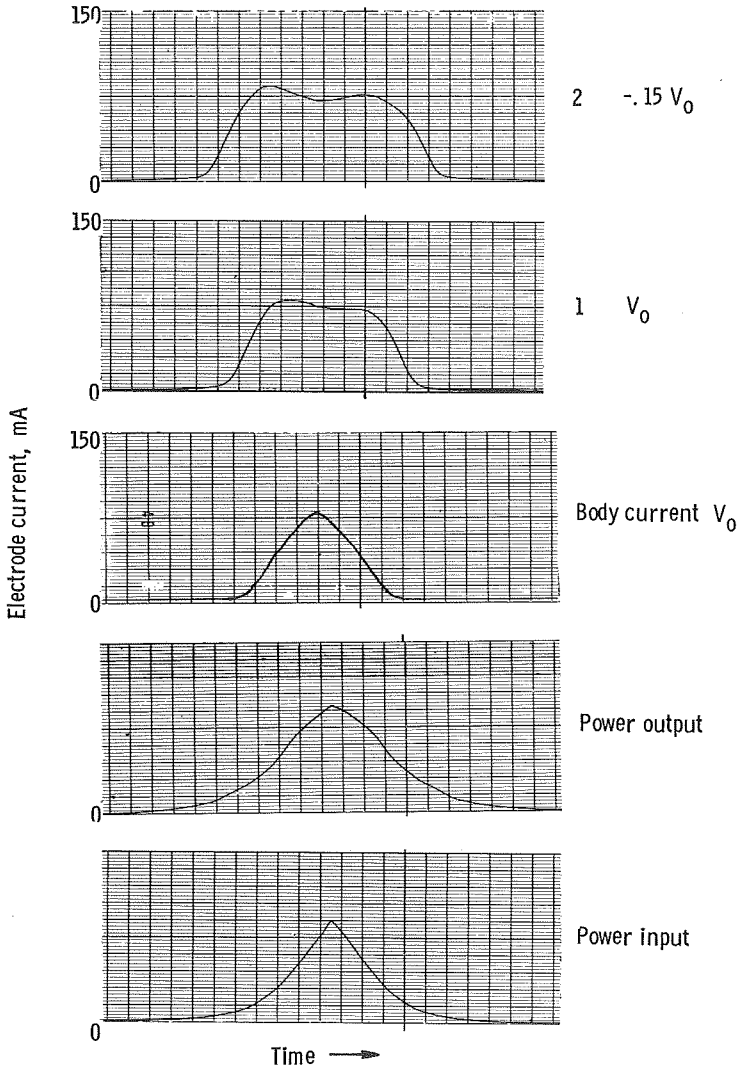

Figure 12. - Variation of electrode currents as a function of drive power.

electrons which make up the beam are changed. Some electrons are accelerated by the rf fields causing an increase in current to electrodes 6, 7, and 8. At maximum power output the majority of electrons have given up kinetic energy and have lower velocities upon entry into the collector. This causes the increase in currents to electrodes 1, 2, 3, and 4 and the increase in current to the body.

At low rf power output levels the beam is diverged primarily by space charge forces. As power output is increased, the beam is converged by the rf field and diverged by space charge forces. The field component normal to the beam axis reverses at the gap center as shown in figure 13, which is an instantaneous picture of the fringing

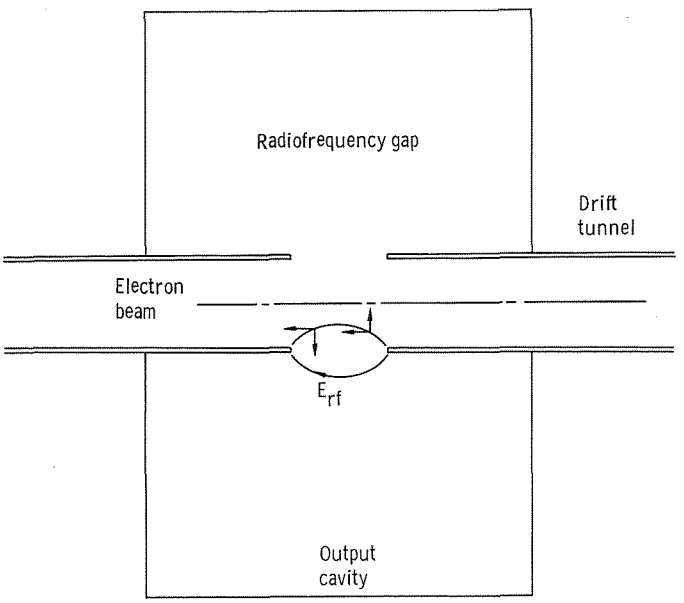

Figure 13. - Radiofrequency field components in output gap.

rf electric field during the deceleration of electrons in the output gap. This causes a convergence of the beam. Since the electrons spend a longer time in the convergent half of the output gap, the net effect is a convergence of the beam by the rf field. Also during the time that the electrons see an accelerating field in the output gap, a convergence of the beam takes place. Electron trajectories through the rf gap have been computed (unpublished NASA data by H. Kosmahl of Lewis Research Center) and are shown in figure 14.

There is no focusing of the beam beyond the entrance to the last cavity. As a result, the interception in all ESFK tubes is high when operating near saturated power levels. There was no attempt made to refocus the beam into the collector region.

In all nonperiodically focused tubes the drift tunnels and cavity lengths may be de-

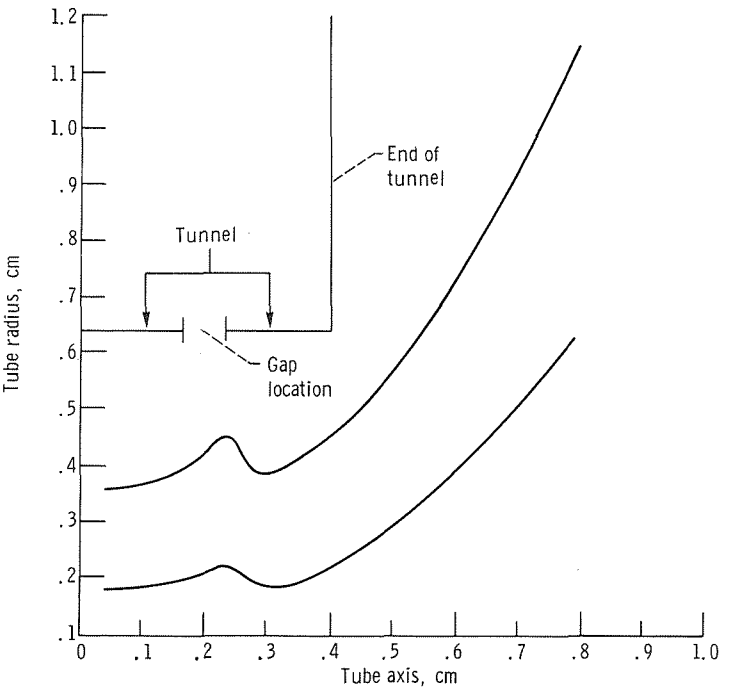

Figure 14. - Electron trajectories through radiofrequency gap.

signed according to rf requirements (e.g., for maximum efficiency). Periodic focusing constrains the tunnels to be of equal lengths. The resulting electronic efficiency of ESFK's is smaller than that in magnetically focused klystrons (MFK's) because the fundamental normalized rf current $i_1 = I_1/I_o$ is of the order of 1.1 to 1.2 while the corresponding value in MFK's may approach 1.7 to 1.8. The power extraction from output cavities is proportional to the product $v_1 i_1$, where $v_1 = \alpha_1 V_o$ is the rf peak voltage in the output cavity. To maximize the power output, α_1 in ESFK's is usually pushed to the limit ($\alpha_1 = 1.1$), at which level the reflection of some electrons sets in. In this ESFK, α_1 is 1.1. Thus, the spent beam of all klystrons and this ESFK in particular have a high percentage of extremely slow electrons which are not well suited for collection at depressed potentials. In addition, a large part of these slow electrons is intercepted beyond the output gap in this ESFK. This would not occur in an MFK.

Calculation of Efficiencies

Figure 15 depicts the overall efficiency of the tube η_o with and without depressed collector operation and the collector efficiency η_c plotted against rf output level P_o.

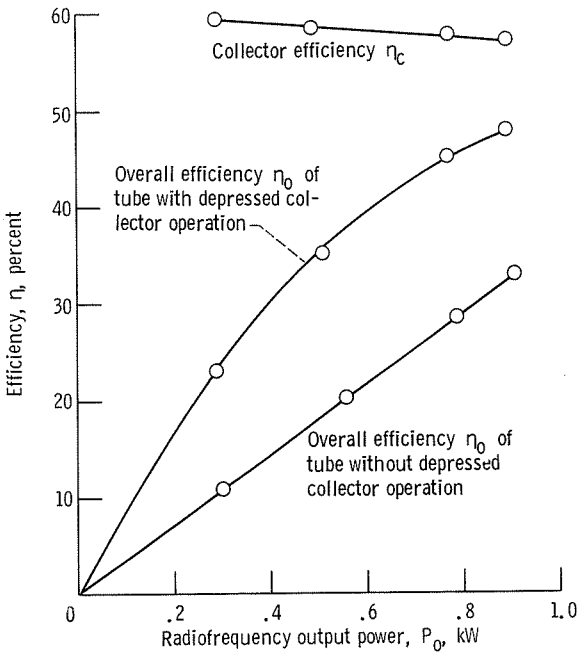

Figure 15. - Efficiency plotted against rf output power delivered to load. (Experimental results.)

In figure 15, the following equations apply:

$$\eta_o = \frac{P_o}{V_o I_b + \sum_n (V_o + V_n) I_n} \tag{1}$$

$$\eta_c = \sum_n \left(\frac{-V_n I_n}{P_S} \right) \tag{2}$$

$$P_o = P_{rf} \eta_{ckt} \tag{3}$$

where

P_o rf output power delivered to load

V_o tube body potential with respect to cathode

I_o cathode current

I_b body current

V_n n^{th} collector electrode potential with respect to the tube body

I_n current to n^{th} collector electrode

P_S spent beam power

P_{rf} rf power generated by tube

η_{ckt} circuit efficiency of tube (95 percent for this ESFK)

Figure 16 is a plot of the spent beam power P_S entering the collector region against the output power. These data were obtained calorimetrically from a single-stage electrically isolated, water cooled collector operated at V_o. The data was then applied to calculate the collector efficiency of the depressed collector. The maximum overall efficiency was increased from 33 to 48 percent at a collector efficiency of 57 percent.

Figure 16. - Calometric measurement of spent beam power.

Experimental results show that there was little or no current going to the patches on the underside of the electrodes and all the current was being collected on top of the electrodes. This indicates that some electrons are being turned around and actually accelerated to electrodes other than the one immediately below the apex of their trajectories. This condition constitutes a decrease in achieved collector efficiency caused by collector apertures which are too large.

Another loss mechanism in the collector is the amount of energy to accomplish velocity sorting. The amount of this energy is defined as the difference between the volt energy at the apex and the initial energy at entry into the collector.

A third loss in collector efficiency is due to electrons which are collected on the lower side of the plate and produce secondary electrons. These electrons are accelerated by the field between electrodes and result in a decrease is achieved efficiency.

A fourth loss is the use of a finite number of collector electrodes which causes most electrons to be collected at points other than the apex of their reajectories. These electrons will be collected with velocities greater than their minimum velocity.

The results obtained can be summarized as follows:

Overall efficiency η_o with depressed collector, percent	48
Overall efficiency η_o without depressed collector, percent	33
Collector efficiency, η_c, percent	57
Radiofrequency output power, P_{rf}, W	935
Spent beam power, P_S, W	1337
Intercepted body power, W	423
Beam power, V_oI_o, W	2695
Power reduction using collector, $\sum V_nI_n$, W	765

For this tube with a P_{rf} of 935 watts and a η_{ckt} of 95 percent, the spent beam power measured calorimetrically is 1337 watts. The body interception power of 423 watts represents electrons impinging with an average electron energy of 0.7 V_o. It is believed that a large amount of electrons with substantial energies are hitting the bottom of plate 1 which is at tube body potential. These electrons are not acted on by the collector and together with the electrons impinging on the body of the tube constitute the major limit in the increase in overall efficiency. The improvement in efficiency was obtained in spite of a body current of 25 percent I_o. This high body current was attributed primarily to limitations of the electrostatic focusing scheme. In this experiment there was no attempt to refocus the beam after it left the output cavity.

It is anticipated that losses in the collector can be reduced and that an ultimate collector efficiency of 75 percent or greater is possible for a ten-electrode (or more) collector. It is expected that this will increase the overall efficiency η_o of the ESFK to between 56 and 59 percent.

If this concept were used on a magnetically focused tube which has very little body current and whose spent beam can be focused into the collector region, the projected overall efficiency η_o would be between 74 and 80 percent.

Effect on Radiofrequency Spectrum

Improvement in the overall tube efficiency through the use of depressed collectors must not be achieved at the price of a poor quality (noisy) rf output spectrum. Such effects occurred frequently with the use of previous depressed collectors which did not prevent backstreaming of primary and secondary electrons. Figure 17 shows output

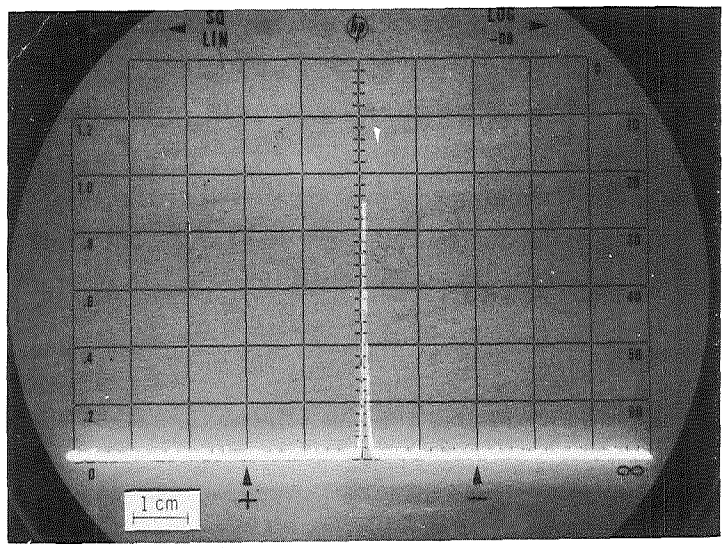

Figure 17. - Output power spectrum obtained with conventional undepressed collector. Radiofrequency output power, P_o = 890 watts; horizontal scale, 3 megahertz per centimeter.

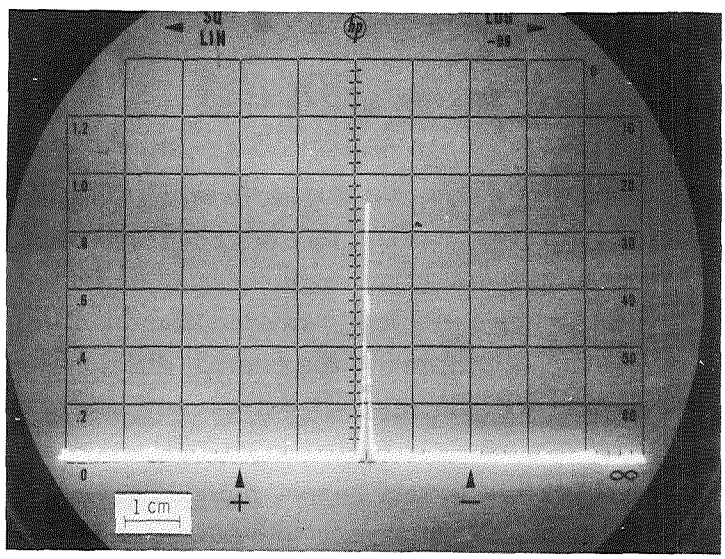

Figure 18. - Output power spectrum obtained with depressed collector. Radiofrequency output power, P_o = 890 watts; horizontal scale, 3 megahertz per centimeter.

frequency spectrum obtained using a conventional undepressed collector. Figure 18 shows output spectrum obtained with the multistage depressed collector. The spectrum analyzer bandwidth used was 10 kilohertz. It can be seen by comparison that there are no spurious signals or noise in the output caused by the depressed collector. Figure 19 is a plot of the AM and FM noise below carrier present in the output signal. These data were obtained utilizing a wave analyzer.

The aforementioned measurements demonstrated that the tube operating with a depressed collector is free of spurious modulation due to ion oscillation in the beam or interference by electrons reflected from the collector into the output cavity.

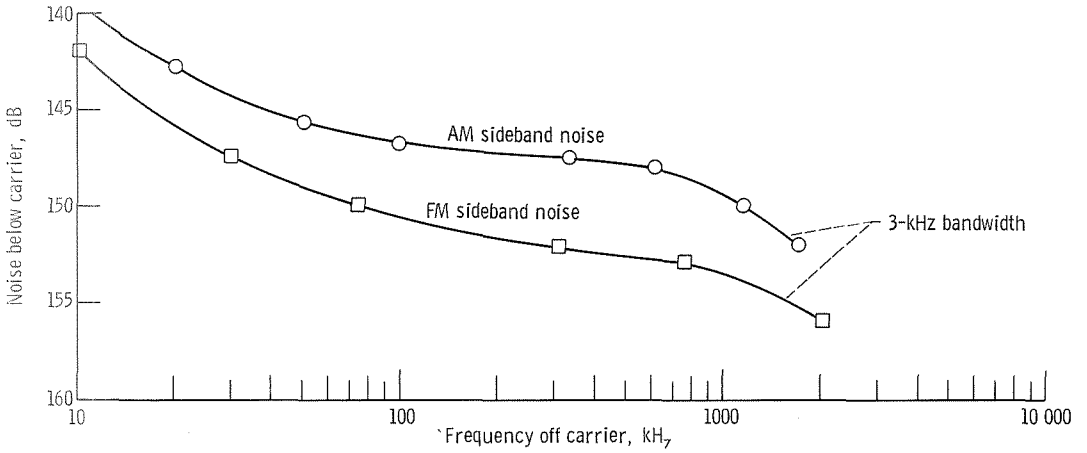

Figure 19. - AM and FM sideband noise with depressed collector.

CONCLUDING REMARKS

Although the initial collector design was tested on an ESFK, the design is also compatible with magnetically focused tubes. One way to extend the results to magnetically focused tubes would be to carefully shield the collector region from the focusing field.

Improved collector designs are expected to raise collector efficiencies to 75 percent or more and promise to significantly improve the overall efficiency of microwave tubes (even those with high electronic efficiencies) without the adverse effects experienced with previous designs.

Although the collector described in this report was designed primarily for use with a space tube, its terrestrial applications appear to be significant. Such a collector could drastically reduce the cost of operation of microwave tubes used in high power applications such as radars, commercial television transmitters, and particle accelerators.

SUMMARY OF RESULTS

The following is a list of the most important results obtained from the experimental evaluation of a multistage depressed collector on an electrostatically focused klystron.

1. It has been demonstrated that an axisymmetric, electrostatic, depressed collector has increased the overall efficiency of an electrostatically focused klystron from 33 to 48 percent.

2. The collector efficiency at saturation was 57 percent.

3. The tube performed normally while being operated with the depressed collector. There were no spurious oscillations due to ions or to electrons reflected into the output gap. The phase characteristics were uniform and behaved as predicted.

4. The basic limitation of this tube for high efficiency is the large (25 percent) intercepted current at saturation. This current never reaches the collector and therefore the collector cannot recover any of the kinetic energy.

Lewis Research Center,
National Aeronautics and Space Administration,
Cleveland, Ohio, April 21, 1971,
164-21.

REFERENCES

1. Neugebauer, W.; and Mihran, T. G.: Multistage Depressed Electrostatic Collector for Magnetically Focused Spaceborne Klystrons. General Electric Co. (NASA CR-72767), Sept. 14, 1970.

2. Mihran, T. G.; and Neugebauer, W.: Analytic Study of a Depressed Collector for Linear Beam Microwave Amplifiers. General Electric Co. (NASA CR-72768), July 8, 1970.

3. Kosmahl, Henry G.: A Novel, Axisymmetric, Electrostatic Collector for Linear Beam Microwave Tubes. NASA TN D-6093, 1971.

NASA-Langley, 1971 — 9 E-6224

NATIONAL AERONAUTICS AND SPACE ADMINISTRATION
WASHINGTON, D. C. 20546

OFFICIAL BUSINESS
PENALTY FOR PRIVATE USE $300

FIRST CLASS MAIL

POSTAGE AND FEES PAID
NATIONAL AERONAUTICS AND
SPACE ADMINISTRATION

POSTMASTER: If Undeliverable (Section 158 Postal Manual) Do Not Return

"The aeronautical and space activities of the United States shall be conducted so as to contribute . . . to the expansion of human knowledge of phenomena in the atmosphere and space. The Administration shall provide for the widest practicable and appropriate dissemination of information concerning its activities and the results thereof."

—NATIONAL AERONAUTICS AND SPACE ACT OF 1958

NASA SCIENTIFIC AND TECHNICAL PUBLICATIONS

TECHNICAL REPORTS: Scientific and technical information considered important, complete, and a lasting contribution to existing knowledge.

TECHNICAL NOTES: Information less broad in scope but nevertheless of importance as a contribution to existing knowledge.

TECHNICAL MEMORANDUMS: Information receiving limited distribution because of preliminary data, security classification, or other reasons.

CONTRACTOR REPORTS: Scientific and technical information generated under a NASA contract or grant and considered an important contribution to existing knowledge.

TECHNICAL TRANSLATIONS: Information published in a foreign language considered to merit NASA distribution in English.

SPECIAL PUBLICATIONS: Information derived from or of value to NASA activities. Publications include conference proceedings, monographs, data compilations, handbooks, sourcebooks, and special bibliographies.

TECHNOLOGY UTILIZATION PUBLICATIONS: Information on technology used by NASA that may be of particular interest in commercial and other non-aerospace applications. Publications include Tech Briefs, Technology Utilization Reports and Technology Surveys.

Details on the availability of these publications may be obtained from:

SCIENTIFIC AND TECHNICAL INFORMATION OFFICE

NATIONAL AERONAUTICS AND SPACE ADMINISTRATION

Washington, D.C. 20546